

Exergy Approach to Decision-Based Design of Integrated Aircraft Thermal Systems

R. S. Figliola*

Clemson University, Clemson, South Carolina 29634-0921

R. Tipton†

Lockheed Martin Aeronautics, Marietta, Georgia 30063

H. Li‡

Clemson University, Clemson, South Carolina 29634-0921

The concept of using an exergy-based approach as a thermal design methodology tool for integrated aircraft thermal systems is introduced. An exergy-based approach was applied to the design of an environmental control system (ECS) of an advanced aircraft. Concurrently, a traditional energy-based approach was applied to the same system. Simplified analytical models of the ECS were developed for each method and compared to assess the ability of each method to suggest optimal design paths. The study identified some roadblocks to assessing the value of using an exergy-based approach: Energy and exergy methods seek answers to different questions, making direct comparisons awkward, and high-entropy generating devices can dominate the design objective of the exergy approach. Nonetheless, exergy methods do approach design differently, providing a ready estimate for efficiency on a component and system basis. Multiobjective optimization tradeoff studies between design weight and entropy generated were used to determine optimal design points. The results from the two analyses provide similar but different decision solutions. The methodology and its implementation are illustrated.

Introduction

IN thermal systems, decisions are based, in part, on the thermodynamic behavior of the component or system. Traditional design procedures use an energy-based approach for decision making. Essentially, this is a thermodynamic first-law analysis. Exergy-based methods deal with the simultaneous application of the thermodynamic principles of the first law and second law to component or system design. Exergy analysis yields an optimal solution based on an objective of entropy generation minimization. Energy-based methods are built on the fundamental concept that energy flows into and out of a system through heat transfer, work, and mass flow. That energy must be conserved is the basic premise of the first law. On the other hand, exergy represents the ability to do work or, put in a different way, the ability to bring about a desired change. Exergy is not conserved and, in fact, is partially or totally destroyed. The amount of exergy destroyed is proportional to the amount of entropy generated. It is the destroyed exergy that brings about the component or system inefficiency. Hence, a design process based on minimizing entropy generation, which reduces exergy destruction to improve efficiency.

The exergy concept can be applied to the optimal design of systems. There are two levels of design where this can be applied: architectural system design, where the basic system form is established, and detail system design, where the subsystems and components are specified. In architectural system design, exergy methods may be advantageous in guiding the conceptual design process that configures the system. In this manner, form and function flow out of a best use of energy framework. Indeed, most biological and natural systems have evolved based on the same concept of minimizing energy waste, and future aircraft should benefit from this viewpoint. In

detail system design, exergy methods may be advantageous in determining the best operating conditions or better component selection. In this manner, the system can reduce parasitic losses and make the best use of available energy. This paper explores the latter case.

Exergy-based methods applied to the design of aircraft integrated systems have been discussed as having advantages over traditional methods. The approach has been applied to components and to land-based power plant design (for example, Refs. 1–3). Tipton et al.⁴ and Figliola and Tipton⁵ first applied exergy methods to the environmental control system of an aircraft. An attempt is made to meet design objectives that make the best use of available energy by looking at the irreversibilities associated with the entropy generation of each component. An attractive feature of the method comes from entropy as a property. Irreversibility within a system is related to the sum of the entropy generated by each component in the system. Constraints, such as size or weight, are readily imposed. However, the demonstration of a completely optimized design of an aircraft system using exergy methods has not been documented.

The original motivation for this work was prompted by a study made to evaluate the aircraft-level impact of using spray-cooling technology in an avionics chassis, which was part of the environmental control system (ECS) of an advanced aircraft.⁴ More recently, participants at U.S. Air Force sponsored workshops⁶ identified several unresolved questions of importance in moving toward an innovative, fully integrated design methodology for air vehicles. Of these, an unambiguous demonstration of exergy-based methodology advantages at the system and aircraft levels was a priority. This paper explores that concept of using an exergy-based method as a thermal design methodology tool for integrated aircraft thermal systems.

Approach

A conventional energy analysis of an integrated system involves a first-law, thermodynamic energy analysis performed on a component-by-component basis throughout the system. Components included consist of heat exchangers, including ram air loss, turbomachine devices, throttle devices, sprayers, combustors, and plumbing. Changes in the system properties are related to changes in energy. System performance is determined for a given set of operating conditions. As an example, the first law applied in a control volume analysis has the form

Received 25 January 2001; revision received 16 August 2002; accepted for publication 16 August 2002. Copyright © 2002 by the American Institute of Aeronautics and Astronautics, Inc. All rights reserved. Copies of this paper may be made for personal or internal use, on condition that the copier pay the \$10.00 per-copy fee to the Copyright Clearance Center, Inc., 222 Rosewood Drive, Danvers, MA 01923; include the code 0021-8669/03 \$10.00 in correspondence with the CCC.

*Professor, Department of Mechanical Engineering. Member AIAA.

†Engineer, Utility Subsystems Integration.

‡Research Assistant, Department of Mechanical Engineering.

$$\frac{dE}{dt} = \sum (\dot{Q} - \dot{W}) + \sum_{in} \omega h - \sum_{out} \omega h \quad (1)$$

where ω is mass flow rate, h is enthalpy, Q is heat transfer, and W is work. The optimal design of the system is determined by variation of appropriate parameters in an effort to minimize an objective function, such as to minimize energy usage [or, equivalently, for aircraft, to minimize the gross takeoff weight (GTW)]. For example, in aircraft systems, an optimal design may correspond to minimizing fuel or weight, or it can be related back to minimizing drag. The controlling variables of the design process reduce to weight, engine power extraction to drive the necessary components, and drag, with constraints such as size imposed. A final review is made to ensure that the optimum design satisfies all of the performance requirements of the system for a given application. Because this method is the conventional analysis, we will not go into detail on its approach.

An exergy analysis of an integrated system incorporates second-law concepts into the analysis on a component-by-component basis in terms of each component's entropy generation. Entropy generation relates to losses or energy waste, that is, irreversibility. Changes in the system can be related to changes in entropy. The attractive feature of such an analysis lies in the physical attributes of entropy as a property: The total entropy generation of each subsystem is simply the sum of the individual entropy generations of each component within the particular subsystem.⁷ Similarly, the total entropy generation of the overall system is determined from the summation of the individual entropy generations of each subsystem. Therein lies an advantage to this method, in that inefficiency can be readily quantified and audited. Thus, this type of analysis results in a common measurement of inefficiency for each of the components in the system, thereby disclosing the problem areas of the system that can be improved. It can be expanded to include manufacturing and maintenance efficiencies. Furthermore, it should provide a basis to compare systems that are quite different in a physical sense, such as structural, power, and aerodynamic systems. An objective for the optimal design is to minimize the entropy generation (or minimize exergy destruction) of the system.

For purposes of estimating component or subsystem irreversibility for open systems, it is convenient to write the second law in the form of entropy generation⁸ for a control volume analysis as

$$\dot{S}_{gen} = \frac{\partial s}{\partial t} - \frac{\dot{Q}}{T} + \sum_{out} \omega s - \sum_{in} \omega s \geq 0 \quad (2)$$

where s is entropy and T is temperature. This defines the rate of entropy generation across the component or subsystem being evaluated. For example, within all connecting ducts and pipes, entropy generation is related to pressure drop and friction losses and can be modeled as

$$\dot{S}_{gen} = (\omega/\rho T)\Delta p \quad (3)$$

and, within heat exchangers, by temperature and flow work potentials by a form of

$$\dot{S}_{gen} = \omega c_p \ln(T_{out}/T_{in})_1 + \omega c_p \ln(T_{out}/T_{in})_2 - \omega R \ln(p_{out}/p_{in})_1 - \omega R \ln(p_{out}/p_{in})_2 \quad (4)$$

where subscripts 1 and 2 refer to the mass streams. Combining Eqs. (1) and (2) yields a basis for exergy analysis

$$\dot{W}_{rev} - \dot{W} = T_0 \dot{S}_{gen} \quad (5)$$

where the reversible work W_{rev} is determined in the limit as the entropy generation is taken to zero. Thus, the rate of thermodynamic irreversibility in an engineering system is directly related to lost or wasted useful power. The system irreversibility is related to the net entropy generation rate for the system and a reference temperature T_0 , for example, environment absolute temperature.⁸ The analysis reduces to one of minimizing entropy generation within imposed constraints. It will suffice to calculate the rate of entropy generation

in comparing various system configurations for an optimal solution. Thus, by estimating the entropy generation of a component, it is possible to determine its contribution to the total irreversibility of the system.⁹

To accomplish the entropy generation analysis of an overall system, an entropy generation number has been developed as the nondimensional form of the rate of entropy generation. A number of approaches for estimating this number have been used (for example, Refs. 1, 3, 7, 10–12), but they all serve the same purpose. Here, we normalize the rate of entropy generation with respect to the heat transfer and junction temperatures associated with the particular device to create an entropy generation number N_s . A typical form is

$$N_s = \frac{T}{q'} \frac{d\dot{S}}{dx} = \frac{\omega}{\rho q'} \left(-\frac{dP}{dx} \right) + \frac{\Delta T}{T} \left(1 + \frac{\Delta T}{T} \right)^{-1} \quad (6)$$

where q' is heat flux, ρ is a fluid density, dP/dx is a pressure drop, and ΔT is a temperature drop across a component. This approach is applied to each component and connecting ductwork. This equation is composed of two parts: one due to a friction pressure drop and one due to heat transfer across a finite temperature difference. When applied to a particular component or subsystem in the design stage, the effects of these two terms oppose one another. Consequently, it is possible to determine an optimal design, or range of optimum designs, of each component based on this concept of entropy generation minimization. This approach will result in a common measurement of inefficiency for each of the components in the system, each described by its N_s , thus, disclosing problem areas that could be improved with the joint objective of minimizing the GTW of the aircraft.

System Model

A model of the ECS of an advanced aircraft, which encompasses seven integrated subsystems, was developed by Tipton et al.⁴ and Figliola and Tipton.⁵ A simplified schematic of the coupled subsystems and components that comprise a typical ECS are shown in Fig. 1. In this example, the ECS analytical model for each subsystem was coded, and its computational engine currently resides behind a spreadsheet-style user interface. Numerical data were easily linked as well. An example of the user interface is shown in Fig. 2. All thermodynamic properties and energy and exergy evaluations required in the analysis for the various subsystems of the ECS are either derived in separate algorithms or obtained from manufacturers and are linked to the model.

The model includes a methodology to analyze each subsystem, component by component, for each separate mission aspect, or as integrated over the mission. In this paper, only the cruise portion of the mission is reviewed. The results of the energy analysis are to determine ultimately the fuel penalty or GTW associated with the system. The results of the exergy analysis are used to reduce N_s for the system while satisfying the mission performance requirements of the ECS. All variables can ultimately be expressed in terms of weight, drag, or engine power or bleed extraction as described in Refs. 13 and 14. Last, multiobjective optimization decision-based approaches are applied in a tradeoff study between these two objectives.

In Fig. 1, the seven integrated subsystems are defined within the model with respect to the aircraft ECS as the 1) cold poly- α -olefin (PAO) loop, 2) vapor cycle system, 3) air cycle system, 4) hot PAO loop, 5) oil loop, 6) hydraulic system, and 7) fuel loop.

In Fig. 1, a spray-cooled avionics chassis was considered to be located within the cold PAO loop of the system, in which PAO is the coolant used in this closed-circuit liquid loop. To model this subsystem, the cooling requirements of the avionics box, such as the fixed junction temperature and heat load, are first given as initial or boundary conditions to the closed loop. Also, the mass flow rate of the coolant is assumed from the ECS performance on a typical advanced aircraft. Even though this flow rate is constant throughout the loop, it was treated as one of the many optimization parameters of the overall system. The pump power required to drive the coolant around the loop is calculated from the pressure drop in the liquid line, including the losses associated with the avionics box and the

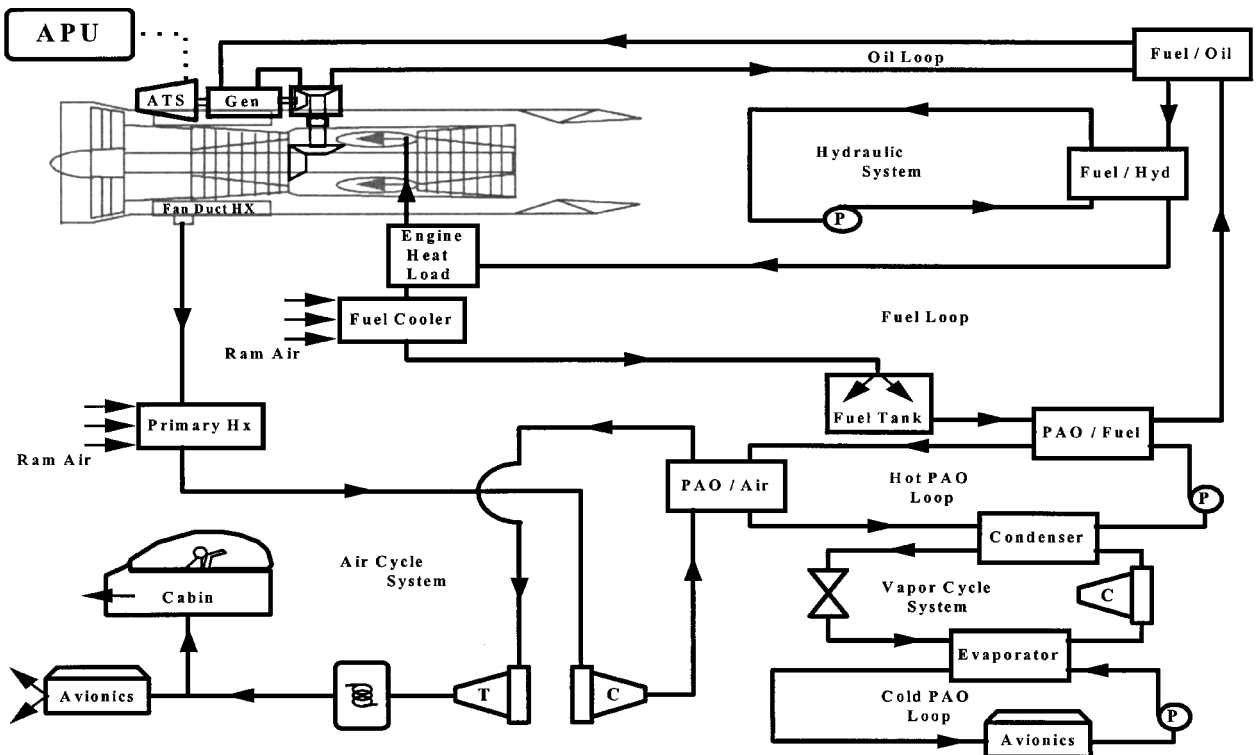


Fig. 1 Schematic of the environmental control system on an advanced aircraft.

	L_c cold (in)	L_c hot (in)	L_c free (in)	$G_{e,c}$ cold (lb/in ² -min)	$G_{e,c}$ hot (lb/in ² -min)	h_c cold (Btu/hr-ft ² -F)	h_c hot (Btu/hr-ft ² -F)	ΔP_c cold (psi)	ΔP_c hot (psi)	UA_{tot} (Btu/hr-F)	NTU	ϵ	Duty (Btu/min)	Weight (lb)
evap.	10.3	10.3	8.1	2.7	11.1	200.0	188.3	0.1	0.8	17886.5	1.6	0.8	2981.6	77.6
cond.	9.8	9.8	7.1	8.6	3.3	189.2	150.0	0.3	0.0	12256.8	1.6	0.8	4453.8	63.7
x2 pao / fuel	7.1	7.1	7.1	5.9	11.9	181.6	217.9	0.0	0.3	7479.3	2.1	0.8	2446.7	38.1
x2 cooler	2.8	13.9	12.2	1.5	5.2	41.7	160.6	1.0	0.1	3384.9	2.4	0.8	6958.6	44.4
TOTAL														306.4

τ (hr)	Mach #	Alt. (ft)	ω_{ram} (lb/min)	$T_{ram,i}$ (F)	$T_{ram,e}$ (F)
1.33	0.90	45000	98.2	-70	226

Wght (lb)	Ram (lb)	Pwr (lb)	CTW (lb)
67.8	97.7	29.4	195.0

Station #	Fluid State	ω (lb/min)	T (F)	P (psia)	h (Btu/lb)	s (Btu/lb-R)
1	liquid	350.0	86.0			
2	liquid	350.0	86.7			
3	liquid	350.0	70.6			
4	two-phase	86.4	175.5	332.7	51.2	0.0960
5	sup. vap.	86.4	66.6	80.5	51.2	0.1021
6	sup. vap.	86.4	76.6	80.5	85.7	0.1676
7	sat. liq.	86.4	224.0	332.7	102.8	0.1765
8	liquid	112.5	128.7			
9	liquid	225.0	131.5			
10	liquid	225.0	166.7			
11	liquid	112.5	167.4			
12	liquid	111.5	115.0			
13	liquid	111.5	156.9			
14	liquid	111.5	167.3			
15	liquid	111.5	194.6			
16	liquid	45.0	299.5			
17	liquid	66.5	299.5			
18	liquid	66.5	115.0			

Device	S_{gen} (Btu/min-R)	Ns_{gen}
avionics	5.220	1.000
pump 1	0.483	0.092
evap.	0.136	0.026
throttle	0.525	0.101
comp.	0.767	0.147
cond.	0.388	0.074
pump 2	0.281	0.054
pao / air	0.588	0.113
x2 pao / fuel	0.083	0.016
x2 fuel / oil	0.912	0.175
x2 fuel / hyd	2.360	0.452
x2 engine	9.173	1.757
x2 cooler	2.779	0.532

Sub System	S_{gen} (Btu/min-R)	Ns_{gen}
cold pao	0.282	0.054
vapor	0.145	0.028
hot pao	0.075	0.014
fuel	16.961	3.249
TOTAL	17.463	3.346

Heat Load (Btu/min)	ϵ
cond.	4454.8 -0.021
pao / fuel	2446.2 0.024
avionic	2850.0
evap.	2981.6 0.800
cond.	4453.8 0.800
pao / air	350.0
x2 pao / fuel	2446.7 0.800
x2 fuel / oil	625.0
x2 fuel / hyd	1675.0
x2 engine	6450.0
x2 cooler	6958.6 0.800

Work Load (hp)	η
pump 1	3.1
comp.	34.7 0.650
pump 2	2.1
TOTAL	39.9

Flight Condition
<input type="radio"/> Ground Idle
<input type="radio"/> Cruise
<input type="radio"/> Supersonic
<input type="radio"/> Loiter

Refrigerant
<input checked="" type="radio"/> R-12
<input type="radio"/> R-114

Heat Load (Btu/min)	Differ. %
cond.	4454.8 -0.021
pao / fuel	2446.2 0.024

Heat Load (Btu/min)	ϵ
avionic	2850.0
evap.	2981.6 0.800
cond.	4453.8 0.800
pao / air	350.0
x2 pao / fuel	2446.7 0.800
x2 fuel / oil	625.0
x2 fuel / hyd	1675.0
x2 engine	6450.0
x2 cooler	6958.6 0.800

Work Load (hp)	η
pump 1	3.1
comp.	34.7 0.650
pump 2	2.1
TOTAL	39.9

Device	S_{gen} (Btu/min-R)	Ns_{gen}
avionics	5.220	1.000
pump 1	0.483	0.092
evap.	0.136	0.026
throttle	0.525	0.101
comp.	0.767	0.147
cond.	0.388	0.074
pump 2	0.281	0.054
pao / air	0.588	0.113
x2 pao / fuel	0.083	0.016
x2 fuel / oil	0.912	0.175
x2 fuel / hyd	2.360	0.452
x2 engine	9.173	1.757
x2 cooler	2.779	0.532

Sub System	S_{gen} (Btu/min-R)	Ns_{gen}
cold pao	0.282	0.054
vapor	0.145	0.028
hot pao	0.075	0.014
fuel	16.961	3.249
TOTAL	17.463	3.346

<input checked="" type="checkbox"/> Entropy Generation
<input checked="" type="checkbox"/> Update Tables
<input checked="" type="checkbox"/> Hx Sizing
<input checked="" type="checkbox"/> Fuel Penalty
<input type="checkbox"/> Performance
<input type="checkbox"/> Converge_1 Plot
<input type="checkbox"/> Converge_2 Plot
<input checked="" type="checkbox"/> Update Variables

Fig. 2 User design interface for the ECS.

evaporator. Finally, the heat load of the evaporator is determined by summing the heat load of the avionics box and the work load of the pump.

The vapor cycle system comprises four components. R-12 is the chosen refrigerant, based on its top performance in similar analyses done using other refrigerants. An iterative procedure is employed to converge on the size of the heat exchanger needed to ensure that all of the heat load on the refrigerant side of the condenser is transferred

to the liquid side (hot PAO loop). The first step in this convergence procedure is to assume an initial value for the condensing temperature (temperature of the refrigerant at the condenser outlet). Next, following a complete analysis of each of the components within the refrigeration cycle, the condenser load is calculated on both the refrigerant side and the liquid side of the heat exchanger. Depending on the magnitude of the difference between the two calculated condenser heat loads, the condensing temperature is then modified, and

Table 1 Typical heat loads and engine fuel flow rates with mission

Operating condition	Engine flow rate (lb/min) (kg/s)	Engine load (Btu/min) (kW)	Hydraulic load (Btu/min) (kW)	Oil load (Btu/min) (kW)	Air load (Btu/min) (kW)
Ground idle	20 (0.15)	2697 (47.42)	1542 (27.1)	602 (10.59)	570 (10.02)
Cruise	40 (0.30)	6445 (113.3)	1663 (29.2)	620 (10.90)	341 (6.00)
Supersonic	200 (1.51)	14,009 (246.3)	2003 (35.2)	700 (12.31)	566 (9.95)
Loiter	80 (0.60)	5598 (98.44)	1752 (30.8)	490 (8.62)	700 (12.31)

the thermodynamic calculations are repeated until the difference is within some predetermined tolerance or convergence requirement.

The primary purpose of the air cycle system is to provide sufficient cooling to both the cabin of the aircraft and the additional avionics equipment having significantly less power generation than the aforementioned avionics box in the cold PAO loop. To accomplish this, bleed air is extracted from the engine and cooled through an open circuit air loop before it is either ventilated through the cabin or blown over the avionics equipment. The two cooling requirements necessary for modeling this subsystem include the airflow rate and the junction temperature at the air/avionics interface. However, to simplify the results in this paper, the details of the air cycle system are excluded.

The only interface between the air cycle subsystem and the liquid loop occurs in the heat exchanger between the hot PAO loop and the air cycle system. Henceforth, the heat load at this interface (PAO/air heat exchanger) is simply treated as one boundary condition to the hot PAO loop. Typical values for this load were obtained from the ECS performance of an advanced aircraft under four separate operating conditions and are listed in Table 1. These operating conditions have been chosen to represent the flight mission of a typical advanced aircraft and are used in the performance evaluation of the system design.

Similar to the cold PAO loop, the hot PAO loop is also a closed-circuit liquid loop using PAO as the coolant. In addition, the two boundary conditions for this particular subsystem are found to be the heat loads of both the condenser and the PAO/air heat exchanger determined earlier. First, the pump power necessary to drive the fluid through the closed loop is calculated from the total pressure drop through the liquid line, including the three heat exchangers. Next, an iterative procedure is again employed to converge on the size of the PAO/fuel heat exchanger needed to ensure that all of the heat load on the PAO side is transferred to the fuel, which represents the heat sink to the overall system. This procedure is very similar to the one used in the vapor cycle analysis; however, the temperature of the fuel leaving the tank (refer to Fig. 1) is used as the initial condition, rather than the temperature of the PAO in the heat exchanger.

The lubricant used within the closed-circuit oil loop is L7808. The primary importance of this subsystem is to cool the mechanical gearbox and the generators driven by the jet engines, which are used to produce the power required to run such system components as the vapor cycle compressor and the hydraulic pumps. To model this subsystem, a temperature cooling requirement for the mechanical equipment, along with a heat load for the fuel/oil heat exchanger, are necessary for each of the aforementioned operating conditions of the aircraft. Similar to the PAO/air heat exchanger mentioned in the air cycle system discussion, typical values for this heat load were obtained from the ECS performance of an advanced aircraft under the same operating conditions. Finally, this heat generated by the mechanical equipment is transferred to the fuel loop through the fuel/oil heat exchanger.

The oil used in the hydraulic system is 83282. Of primary importance to this subsystem is the cooling of the hydraulic equipment used to operate the landing gear and the flight control surfaces of the aircraft throughout a mission. Again, the details of this subsystem are excluded here, with the exception of its single interface with the fuel loop. Consequently, a temperature cooling requirement, along with a typical fuel/hydraulic (F/H) heat exchanger load for each of the four operating conditions of the aircraft, are necessary for sufficiently modeling the hydraulic system.

The JP4 fuel loop serves as the heat sink for the entire liquid circuit of the ECS. The boundary conditions to this subsystem include

the already determined heat loads from the PAO/fuel heat exchanger, the fuel/oil heat exchanger, the F/H heat exchanger, and the engine heat load. As before, the engine heat loads necessary for a complete analysis of the system were obtained from the ECS performance of an advanced aircraft for each of the aforementioned operating conditions. In addition to the heat loads, limits on the fuel temperature (146–149°C) and an engine fuel flow rate required by the engine are necessary for each of these operating conditions. Average fuel temperatures in the tank were maintained at 46°C.

Together with the boundary conditions of the subsystem, an iterative procedure is used to converge on the sizes of both the fuel/oil and the F/H heat exchangers. Once these two heat exchangers are sized, the fuel flow rate through the fuel cooler (illustrated in Fig. 1) is then determined by subtracting the engine fuel flow requirement from the total fuel flow rate out of the tank. Next, the fuel cooler is sized with an iterative procedure so that the resulting temperature of the fuel entering the fuel tank is equal to the temperature of the fuel leaving the tank. In sizing the fuel cooler, the various altitudes and Mach numbers experienced by the aircraft over an entire flight mission must be taken into account due to their significant influence on the airflow rate through the ram air scoop.

Results and Discussion

In the traditional energy analysis, system performance and component weights can be determined by weighing the cooling requirements of a particular component with the performance requirements of the aircraft. This design approach is similar to the traditional energy conservation methods found in the integrated thermal management procedures currently used by industry. Results of such analyses provide ram airflow/drag measurements, equipment weights, engine horsepower extraction, and engine bleed extraction. In Ref. 13, a corresponding fuel penalty can be calculated for each of the aircraft penalties and summed to determine the total fuel penalty or GTW of the aircraft. (Note, the calculated overall GTW is that due to the systems and variables included in this ECS model, and is not the total GTW of the aircraft.) Next, the optimum design of the overall system can be determined by varying such parameters as heat exchanger effectiveness, heat exchanger size, and ECS coolant flow rate in an effort to minimize the total GTW of the aircraft. Finally, this resulting optimum system design undergoes a performance analysis to determine whether it satisfies all of the aircraft operating conditions in a flight mission typical of an advanced aircraft.

In exergy analysis, each component of the system, including the avionics box, compressor, expansion valve, heat exchangers, and pumps, is evaluated in terms of its entropy generation. Next, due to the physical attributes of entropy as a property, the total entropy generation of each subsystem is found by simply summing the individual entropy generations of each of the components within that particular subsystem. Finally, the total entropy generation of the overall system is determined by summing the individual entropy generations of each of the seven subsystems.

The total GTW, as defined here, refers to the fuel penalty portion associated with operating the system and the fixed component weight portion. The component weights used were representative only. In this paper, the fuel penalty portion of the GTW is composed of four distinct fuel penalties: equipment weight penalty, ram air penalty, bleed air penalty, and shaft horsepower extraction penalty. Consequently, the controlling variables of the design process include the size (or weight) of the three aforementioned heat exchangers, flow rates of both ram air through the fuel cooler and bleed air off of the engine, and power necessary to drive the compressor and the coolant pumps.

A system-level sensitivity analysis of the design based on heat exchanger effectiveness and coolant mass flow rate was performed, with the objective of minimizing either GTW or N_s . Components relevant to this discussion included the evaporator, condenser, PAO/fuel heat exchanger, and fuel cooler and the hot and cold PAO loops. Effectiveness was confined to a range of between $0.50 \leq \varepsilon \leq 0.95$. Mass flow rate was confined to a range of between $125 \leq \omega \leq 425$ lbm/min ($57 \leq \omega \leq 193$ kg/min).

Figures 3 and 4 demonstrate results for the PAO loop shown in Fig. 1 for GTW and for N_s against coolant mass flow. A considerable amount of detail can be extracted from the sensitivity analysis. In Fig. 3a, system GTW is plotted vs cold PAO mass flow rate. A 16% increase in component weight is noted as mass flow rate is increased over its range due to the increased size of the evaporator required to handle this. Although the increased mass velocity improves the heat transfer coefficient, the heat exchanger effectiveness decreases, requiring an increase in heat transfer area and size. However, the shaft horsepower extraction weight penalty was found to decrease, whereas the pump power weight penalty increased. The

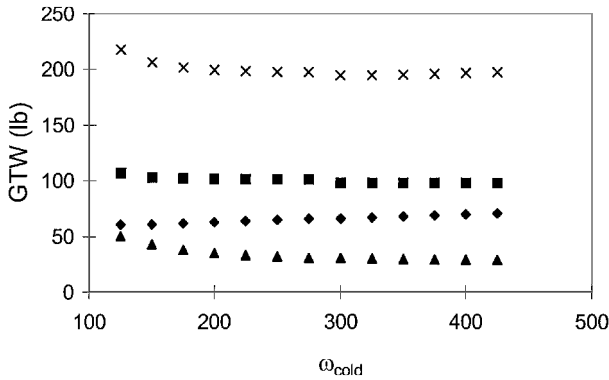


Fig. 3a GTW vs cold PAO mass flow rate: ♦, weight; ■, ram air; ▲, power; and ×, total.

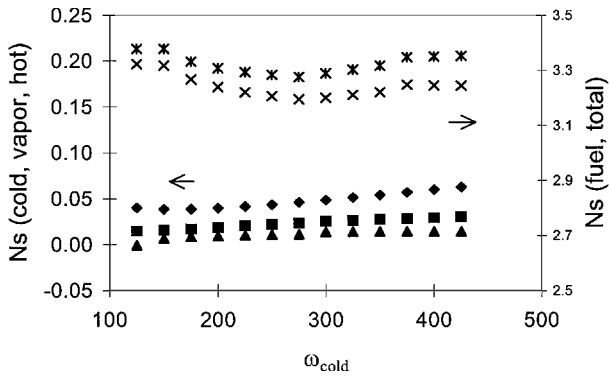


Fig. 3b Entropy generation number vs cold PAO mass flow rate: ♦, cold PAO; ■, vapor; ▲, hot PAO; ×, fuel; and *, total.

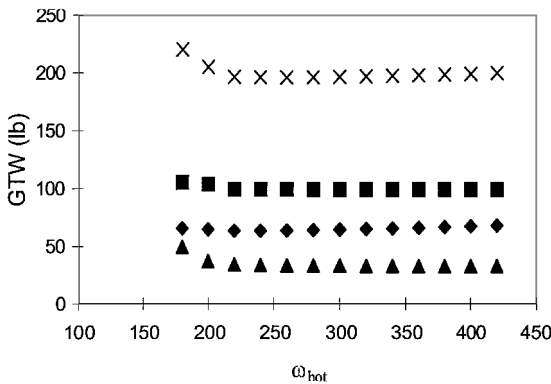


Fig. 4a GTW vs hot PAO mass flow rate: ♦, weight; ■, ram air; ▲, power; and ×, total.

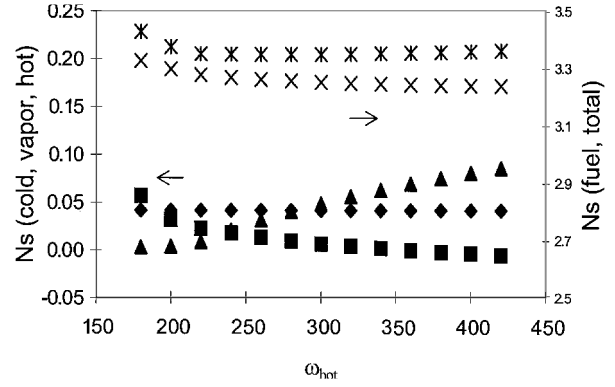


Fig. 4b Entropy generation number vs hot PAO mass flow rate: ♦, cold PAO; ■, vapor; ▲, hot PAO; ×, fuel; and *, total.

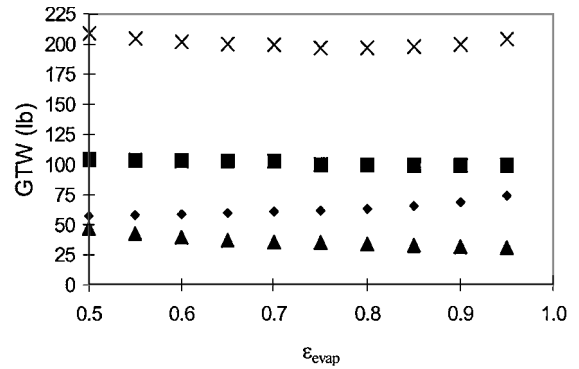


Fig. 5a GTW vs evaporator effectiveness: ♦, weight; ■, ram air; ▲, power; and ×, total.

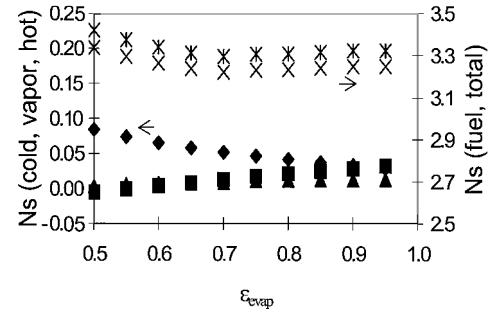


Fig. 5b Entropy generation number vs evaporator effectiveness: ♦, cold PAO; ■, vapor; ▲, hot PAO; ×, fuel; and *, total.

accompanying reduction in condensing temperature with increased mass flow rate lead to a slight decrease in ram air fuel penalty because a reduction in temperature at this point in the cycle subsequently reduces the mass flow rate of fuel necessary to maintain the engine fuel temperature, reducing the required ram air flow rate. In Fig. 3b, the coolant mass flow rate is seen to influence the entropy generation of the system. Interestingly, for the avionics box, the resulting decrease in temperature difference across the box balanced out the increase in entropy generation associated with the increased mass flow. On the other hand, the corresponding increase in temperature difference across the evaporator and the increased pump requirements contributed to entropy increases. At 300 lbm/min, an increase in the mass flow of fuel was required to maintain the engine fuel temperature limit, providing an increase in entropy generation. A minimum in GTW occurs at 300 lbm/min, whereas a minimum in N_s occurs at 275 lbm/min.

Similar detail can be extracted from the results for the hot PAO mass flow rate in Figs. 4a and 4b. Both cases show a rapid drop in GTW and N_s as coolant mass flow is increased to about 260 lbm/min. For flow rates above 260 lbm/min, the GTW remains about constant. Entropy generation sees a moderate increase above 260 lbm/min,

mostly due to higher net losses associated with the higher flow rate and pump requirements against the system gains due to lower temperature differences. A minimum in GTW occurs at 300 lbm/min, whereas a minimum in N_s occurs at 260 lbm/min.

Figures 5 and 6 demonstrate the results for the evaporator and condenser in the PAO loops for GTW and N_s against effectiveness. Figure 5a shows the results for GTW vs evaporator effectiveness. Component weight increases with effectiveness due to the increase in heat exchanger size. However, there is a nearly 35% decrease in shaft power extraction weight penalty as effectiveness increases over the tested range. As evaporator effectiveness increased, the

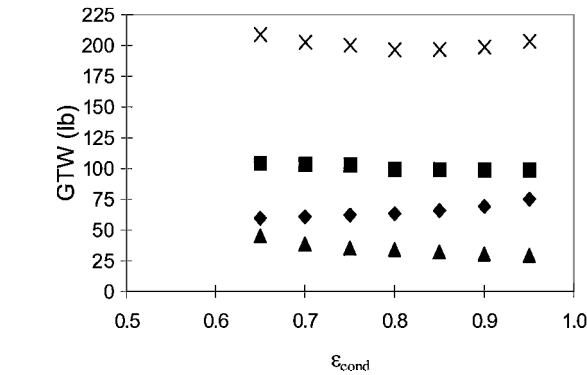


Fig. 6a GTW vs condenser effectiveness: ♦, weight; ■, ram air; ▲, power; and ×, total.

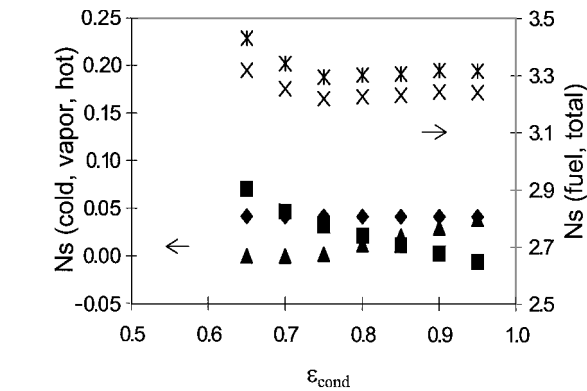


Fig. 6b Entropy generation number vs condenser effectiveness: ♦, cold PAO; ■, vapor; ▲, hot PAO; ×, fuel; and *, total.

condensing temperature of the vapor cycle was found to decrease, reducing the temperature gap between the heat exchangers and reducing the compressor requirements. Figure 5b shows the results for N_s vs effectiveness for the evaporator. N_s decreases with increasing effectiveness through a value of 0.75. Above this value, an increase in the mass flow rate of fuel required to maintain the engine fuel temperature limit lead to an increase in the entropy generation of the system. For each method, a minimum in effectiveness was found at 0.75. Similarly, Figs. 6a and b show the results for GTW and N_s vs condenser effectiveness. In Fig. 6a, the GTW reaches a minimum at an effectiveness of 0.8. In Fig. 6b, N_s reaches a minimum at an effectiveness of 0.8.

The results of the two methods as applied in this study provided similar, but not exact, optimal solutions. Some differences can be attributed directly to uncertainty. As can be seen in Figs. 3–6, high-entropy generating devices have a strong impact on decisions. The combustion and mixing of the fuel has a strong role in computing the entropy generation associated with the system design, whereas it is not directly considered in computing the GTW or fuel penalty of the ECS system. Limiting the uncertainty in the entropy generation estimation is likely to be important in the success of the exergy method, and rigorous methods to evaluate uncertainty exist.¹⁵ In Figs. 3b, 4b, 5b, and 6b, the exergy methods do demonstrate an optimal operating condition, providing a clear decision basis. The energy method results in Figs. 3a, 4a, 5a, and 6a are more vague, relying on the designer's experience for selection.

A pareto optimal design set was generated through the two simultaneous objectives to minimize entropy generation and to minimize GTW. A genetic algorithm was used in this optimization. Figure 7 shows the results of the tradeoff study with each data point designating a unique design solution. The abscissa has been normalized as $1 - x$, where x is the percent fraction between the minimum design weight solution and the heaviest design weight solution. Solutions toward the left side of the plot will weigh GTW more heavily in the tradeoff design, whereas the right-hand side solutions will weigh entropy generation more heavily. Overall, the range of the weights varies by about 8%, suggesting the closeness of the two approaches.

In concept, the design that meets constraints but minimizes entropy generation should yield an optimal solution. A fundamental issue remains that bears on the proposed objectives. When these two approaches are used independently, direct comparisons are difficult to make. Each approach intrinsically asks a separate question; they have different objectives. In the context of the imposed problem concerning ECS design, energy analysis seeks answers to the question: How much additional fuel will it cost to overcome the aircraft penalties imposed by the ECS performance requirements? Its optimal design is the one that imposes the smallest fuel penalty, resulting

Pareto Curve

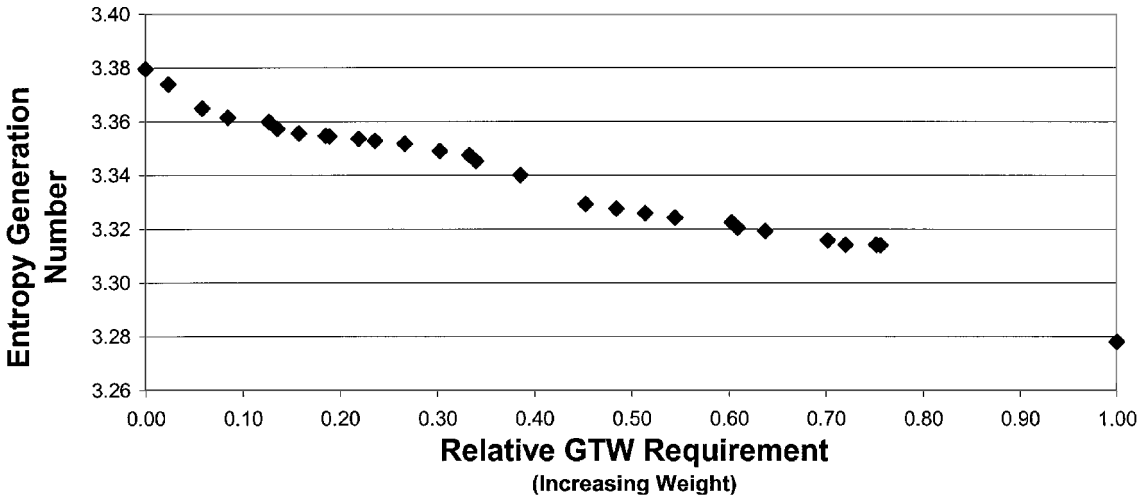


Fig. 7 Pareto optimal design set for the two objectives.

in the minimum GTW, thus leading to the minimum cost. Exergy analysis seeks answers to the question: How much excess fuel is wasted or not utilized to its potential to overcome irreversibilities associated with the ECS design? Irreversibility is associated with wasted energy or destroyed exergy with its associated increase in entropy generation. Its optimal design is the one that minimizes the excess fuel needed to operate the ECS. This work formulates a working demonstration of applying and interpreting exergy analysis as a viable design tool for aircraft systems.

Conclusions

Two methods for analyzing and evaluating the ECS on an advanced aircraft have been compared in this paper. An exergy-based approach was applied to the design of an ECS of an advanced aircraft. Concurrently, a traditional energy-based approach was applied to the same system. Simplified analytical models of the ECS were developed for each method and compared to determine the validity of using the exergy approach to facilitate the design process in optimizing the overall system for a minimum GTW. The study identifies some roadblocks to assessing the value of using an exergy-based approach. The results from the two analyses provided similar, although not exact, solutions and different information. Because energy and exergy methods seek answers to somewhat different questions, direct comparisons are awkward. Also, high-entropy generating devices were seen to dominate the design objective of the exergy approach. Nonetheless, exergy methods do provide decision information to aid design, providing a ready estimate for efficiency on a component and system basis and indicating optimal operating conditions. Further progress is necessary to validate the hypothesis that exergy-based methods are advantageous for the design of integrated systems.

References

- ¹Bejan, A., "Review: The Thermodynamic Design of Heat and Mass Transfer Processes and Devices," *International Journal of Heat and Fluid Flow*, Vol. 8, No. 4, 1987, pp. 258–276.
- ²Bejan, A., "Advanced Energy Systems: Minimizing Entropy in Thermal Systems," *Mechanical Engineering*, Vol. 111, Aug. 1989, pp. 88–91.
- ³Herbein, D. S., and Rohsenow, W. M., "Comparison of Entropy Generation and Conventional Method of Optimizing a Gas Turbine Regenerator," *International Journal of Heat and Mass Transfer*, Vol. 31, No. 2, 1988, pp. 241–244.
- ⁴Tipton, R., Figliola, R. S., and Ochterbeck, J. O., "Thermal Optimization of the ECS on an Advanced Aircraft with an Emphasis on System Efficiency and Design Methodology," SAE Aerospace Systems Conf., SAE Paper 97, May 1997.
- ⁵Figliola, R. S., and Tipton, R., "An Exergy-Based Methodology for the Design of Integrated Aircraft Systems," Society of Automotive Engineers, SAE Paper 2000-01-5527, Oct. 2000.
- ⁶Carter, D., "Energy-Based Design Workshop," U.S. Air Force Research Lab., Rept. AFRL-VA-WP-TR-2001-3003, Dayton, OH, Jan. 2001.
- ⁷Bejan, A., *Entropy Generation Minimization: The Method of Thermodynamic Optimization of Finite-Size Systems and Finite-Time Processes*, CRC Press, New York, 1996, pp. 21–40.
- ⁸Van Wylen, G., Sonntag, R., and Borgnakke, C., *Fundamentals of Classical Thermodynamics*, 5th ed., Wiley, New York, 1998, pp. 272–345.
- ⁹Bejan, A., "General Criterion for Rating Heat-Exchanger Performance," *International Journal of Heat and Mass Transfer*, Vol. 21, No. 5, 1978, pp. 655–658.
- ¹⁰Kotas, T., and Shakir, A., "Exergy Analysis of a Heat Transfer Process at a Subenvironmental Temperature," *Second Law Analysis and Modeling*, AES-3, ASME International, New York, 1986.
- ¹¹Sarangi, S., and Chowdary, K., "On the Generation of Entropy in a Counterflow Heat Exchanger," *Cryogenics*, Vol. 22, No. 2, 1982, pp. 63–65.
- ¹²Sekulic, D. P., "Entropy Generation in a Heat Exchanger," *Heat Transfer Engineering*, Vol. 7, Nos. 1–2, 1986, pp. 83–88.
- ¹³"Aircraft Fuel Weight Penalty due to Air Conditioning," AIR 1168, Vol. 8, *SAE Aerospace Applied Thermodynamics Manual*, Society of Automotive Engineers, SAE International, Warrendale, PA, 1989.
- ¹⁴"Aerothermodynamic Systems Engineering and Design," AIR 1168, Vol. 3, *SAE Aerospace Applied Thermodynamics Manual*, Society of Automotive Engineers, SAE International, Warrendale, PA, 1990.
- ¹⁵Figliola, R. S., and Beasley, D. E., *Theory and Design for Mechanical Measurements*, 3rd ed., Wiley, New York, 2000, pp. 149–183.